IOPscience iopscience.iop.org

Home Search Collections Journals About Contact us My IOPscience

The optical properties of ZnO films grown on porous Si templates

This article has been downloaded from IOPscience. Please scroll down to see the full text article.

2003 J. Phys. D: Appl. Phys. 36 2705

(http://iopscience.iop.org/0022-3727/36/21/017)

View the table of contents for this issue, or go to the journal homepage for more

Download details:
IP Address: 159.226.165.151
The article was downloaded on 10/09/2012 at 05:00

Please note that terms and conditions apply.

INSTITUTE OF PHYSICS PUBLISHING JOURNAL OF PHYSICS D: APPLIED PHYSICS

J. Phys. D: Appl. Phys. **36** (2003) 2705–2708 PII: S0022-3727(03)66538-1

The optical properties of ZnO films grown on porous Si templates

Y L Liu[1], Y C Liu[1,2,3], H Yang[2], W B Wang[1], J G Ma[1], J Y Zhang[1], Y M Lu[1], D Z Shen[1] and X W Fan[1]

[1] Key Laboratory of Excited State Process, Chinese Academy of Sciences, Changchun Institute of Optics, Fine Mechanics and Physics, Chinese Academy of Sciences, Changchun 130022, People's Republic of China

[2] Center for Advanced Optoelectronic Functional Material Research, The Northeast Normal University, 130024, People's Republic of China

E-mail: ycliu@nenu.edu.cn

Received 23 July 2003
Published 15 October 2003
Online at stacks.iop.org/JPhysD/36/2705

Abstract

ZnO films were electrodeposited on porous silicon templates with different porosities. The photoluminescence (PL) spectra of the samples before and after deposition of ZnO were measured to study the effect of template porosity on the luminescence properties of ZnO/porous Si composites. As-prepared porous Si (PS) templates emit strong red light. The red PL peak of porous Si after deposition of ZnO shows an obvious blueshift, and the trend of blueshift increases with an increase in template porosity. A green emission at about 550 nm was also observed when the porosity of template increases, which is ascribed to the deep-level emission band of ZnO. A model-based band diagram of the ZnO/porous Si composite is suggested to interpret the properties of the composite.

1. Introduction

The study of ZnO has been an area of strong interest in recent years since ZnO has various potential applications in low-voltage and short-wavelength opto-electronic devices such as light emitting diodes and laser diodes. Usually, the photoluminescence (PL) spectrum of ZnO is composed of a visible blue-green band related to deep-level defect emission and ultraviolet emission from free excitons [1]. ZnO has been widely investigated on various substrates [2, 3], or porous templates [4, 5], while ZnO films grown on porous Si templates have been little studied. Porous Si is one of the most important Si-based luminescence materials since Canham presented the first observation of efficient photoluminescence from porous Si at room temperature [6]. Its open structure and large surface area, combined with unique optical and electrical properties, make it a good option for templates [7, 8]. In general, the emission energy of porous Si layers increases with decreasing size, covering the entire visible spectrum from red to blue [9, 10] and the red-emitting PS can be obtained easily. If the red emission from porous Si layers could be combined with a blue-green emission from a ZnO film, it would be possible to obtain white light. This offers a cheap route for a white LED, which is significant for display technology.

In this paper, ZnO polycrystalline thin films have been electrodeposited on porous Si templates with different porosities. High-quality ZnO films electrodeposited on c-Si have been reported in our previous paper [11], which reports the possibility of growing ZnO films on porous Si. The photoluminescence properties of the porous Si before and after deposition of ZnO were studied. When the ZnO/porous Si composite is excited by the 488 nm line of an Ar^+ laser, the emission in the red region from porous Si shows an obvious blueshift compared with as-prepared porous Si templates. The blueshift increases with an increase in template porosity. Accompanying with the blueshift, a new emission on the high-energy side, about 550 nm, related to the deep-level emission of ZnO is observed. In order to explain these experimental results, a model has been proposed to describe the emission mechanism.

2. Experiment

The preparation of the samples involved two steps: first, the preparation of PS templates with strong visible

[3] Author to whom any correspondence should be addressed.

 © 2003 IOP Publishing Ltd Printed in the UK

photoluminescence by anodic etching and second, cathodic electrodeposition of ZnO on the PS templates. PS templates were obtained by electrochemical etching of (001)-oriented n-type Si with resistivity 4–6 Ωcm. The Si wafers were irradiated using a 500 W white light from a distance of 20 cm above the electrochemical cell. The etching was carried out in an HF and C_2H_5OH mixture ($HF : C_2H_5OH = 1 : 1$) at a constant current of 40 mA cm^{-2} for 10, 20, and 30 min. The as-made PS samples were cut into two pieces. One series was labelled as A, B, and C. The other was used to deposit ZnO films immediately. Deposition was carried out in a dimethylsulfoxide solution containing 0.03 M $ZnCl_2$. 0.1 M KCl was introduced to ensure good conductivity of the solution. Electrodeposition was carried out at a constant current of 0.1 mA cm^{-2} for 1 h at room temperature. ZnO film was also grown on crystal Si under the same conditions for comparison. The samples of ZnO films grown on A, B, and C templates were labelled as A1, B1, and C1, respectively.

Cross sectional views of the samples were obtained using a scanning electron microscope (SEM). X-ray diffraction (XRD) spectra of the films were taken on a Siemens D500 diffractometer operating in the θ–2θ Bragg configuration using CuK_α radiation of 1.5418 Å. Raman and PL spectra were measured using a micro-laser Raman spectrometer, and the 488 nm line of an Ar^+ laser was used as an excitation source.

3. Results and discussion

Figure 1 illustrates a typical SEM image of the cross sectional view of the porous Si templates. The pore with a straight parallel channel was perpendicular to the substrate. The average pore diameter is about 500 nm, and the length is about 4 μm. The SEM photographs of the as-prepared porous Si samples show that an increase in etching time leads to creation of more cracks and voids, as well as increases the porosity of the templates.

When ZnO is grown on the porous templates, energy dispersive x-ray spectroscopy shows that the film consists of Zn and O. The diffraction peaks of (100), (002), and (101) have been observed in the XRD patterns, which demonstrates the formation of polycrystalline ZnO films with no preferred orientation on the PS templates.

The Raman spectra of samples A, B, and C were compared with crystal Si, as shown in figure 2. The Raman line at 520 cm^{-1} from crystal Si, which is sharp and symmetric, is attributed to scattering of the first-order phonon. While for porous Si, with an increase in etching time the Raman peak shifts to a lower frequency, which is 515 cm^{-1}, 508 cm^{-1}, and 505 cm^{-1} for samples A, B, and C, respectively, the line width broadens, and the asymmetry of the scatter line strengthens. These changes are attributed to the confinement of the Si nanocrystal. For crystal Si, only a $k = 0$ momentum selection rule of the first-order Raman spectrum can be satisfied, so only one peak at 520 cm^{-1} is observed in the Raman spectrum. As the crystalline size is reduced to nanometres, the $k = 0$ momentum selection rule will be relaxed. The phonon scattering will not be limited to the centre of the Brillouin zone, and phonon dispersion near the zone centre needs to be considered. As a result, the frequency-shift, broadening, and asymmetry of the first-order Raman scattering are observed. The average diameter of Si crystallite spheres, L, can be evaluated from the Raman spectra using a spatial model. In this model, the diameter of nano-Si can be calculated from formula (1) [12]:

$$L = \frac{1}{2}\frac{\exp(-\pi^2)}{(\varpi_L - \varpi_0)^2 + (\Gamma_0/2)} \tag{1}$$

where ϖ_L is the frequency of the crystalline-like mode for a microcrystal size L. ϖ_0 and Γ_0 are 520 cm^{-1} and 4 cm^{-1}, respectively, for crystalline Si. Kanemitsu *et al* [13] have demonstrated that the particle size, L, of various porous Si samples determined from Raman spectra is in good agreement with those sizes experimentally determined using transmission electron microscopy. The average size of nano-Si calculated from formula (1) is 8.9 nm, 1.7 nm, and 1.1 nm for samples A, B, and C, respectively. With an increase in etching time, the size of the Si nanocrystal decreases.

Figure 3 gives the PL spectra of porous Si with different porosities, which also shows the effects of quantum confinement. Two clear trends can be observed from

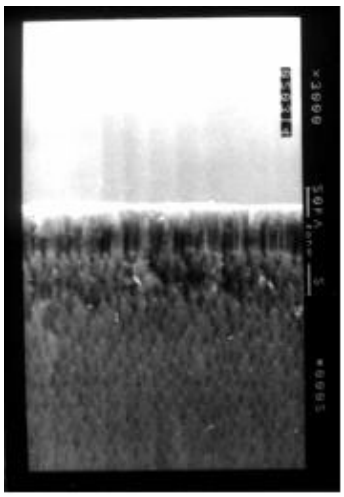

Figure 1. Cross sectional SEM image of sample A.

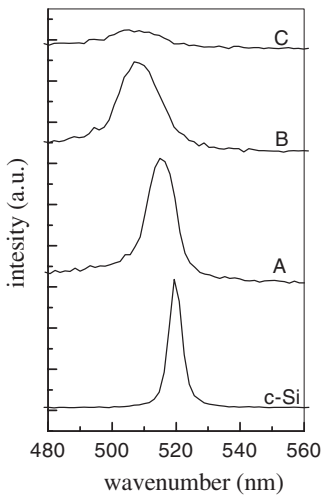

Figure 2. Raman spectra of samples A, B, and C and c-Si.

figure 3: a shift towards a shorter wavelength and an increase in the integrated intensity. The peak at the high-energy side shifts from around 747 nm for sample A to 736 nm for sample C, which is due to the quantum confinement. The band gap of the Si nanocrystal is widened, induced from the quantum effect, which makes the PL spectra move to the visible range. Other peaks at 760, 795, and 879 nm have also been observed in all the three spectra, which are independent on the PS layers. These may be attributed to the surface state emission of the Si nanocrystal.

Figure 4 gives the PL spectra of the porous Si composites after deposition of ZnO. The emission spectrum of sample A1 shows a near-perfect Gauss line with an emission peak at 679 nm. The PL spectrum of sample B1 has a red peak at 644 nm with a weak shoulder at the higher-energy side of about 550 nm. For sample C1, two obvious emission bands can be observed, the red emission band located at 620 nm and another band in the green region, with a maximum at ∼550 nm. After deposition of ZnO, a blueshift of the red emission band occurs compared with the as-prepared porous Si templates. A similar blueshift of porous Si has also been reported after deposition of ZnO by Elhouichet *et al* [14]. A blueshift of porous Si has also been reported for oxidized porous Si in air ambient [10, 15, 16]. The blueshift after deposition of ZnO is 71 nm, 103 nm, and 117 nm, for samples A1, B1, and C1, respectively. The larger the porosity of the template, the greater is the blueshift of the red emission. The red emission band is ascribed to emission from porous Si whose surface was passivated by oxygen due to deposition of ZnO, as will be discussed later. Another feature is evident from the PL spectra: as the porosity of the template increases, the intensity of the red emission decreases while a green band emission at ∼550 nm appears for sample B1 and C1, which may be associated with the deep-level emission of ZnO.

Before interpreting the emission mechanism of the composite system, we should study the emission of ZnO first. ZnO has been known as a luminescent material for a century. Usually two emission bands are found, a narrow UV peak at around 380 nm, due to exciton emission, and a broader emission band situated in the green part of the visible spectrum. The nature of the green emission of ZnO has been the subject of much research and is still controversial and unclear. Copper impurities, chemisorbed oxygen, sulfur impurities, and intrinsic defects such as interstitial zinc ions or oxygen vacancies were assumed to be the recombination centres. During the past years, oxygen vacancies have been assumed to be the most likely candidates for the recombination centres involved in the visible luminescence of ZnO. Recently, Dijken *et al* [17] have demonstrated that the visible emission is due to a transition of a photogenerated electron from a shallow level close to the conduction band edge to a deeply trapped hole (a V_0^{**} centre). The surface-trapped hole can tunnel back into the particle, where it recombines with an electron in an oxygen vacancy (V_0^*), resulting in the creation of a V_0^{**} centre, which is the recombination centre for the visible emission.

Now we go back to the discussion of the PL mechanism of the composite ZnO/porous Si system. ZnO introduced into the PS surface should not influence the Si crystalline size but should change the surface structure, and the interface between ZnO and porous Si plays an important role in the emission process of the composite system. In the light of the observations in this work and previous studies, we explain the experimental results in terms of a model described below and presented by the band energy diagram in figure 5. Here $\chi_{Si} = 4.01$ eV, $\chi_{ZnO} = 4.35$ eV denote the electron affinity of silicon and ZnO. In this model, porous Si is considered as a material that consists of nanocrystal Si with a band gap larger than

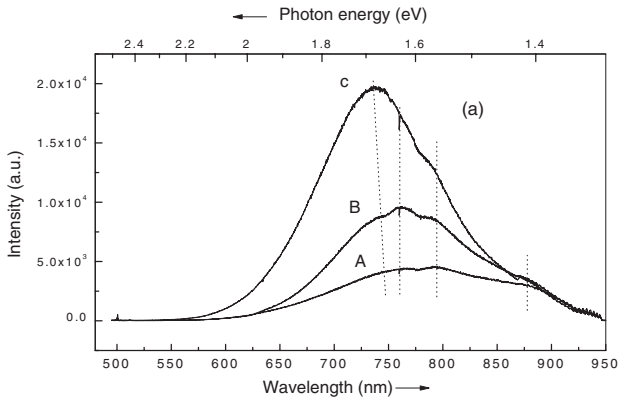

Figure 3. PL spectra of samples A, B, and C, excited by the 488 nm line of an Ar^+ laser.

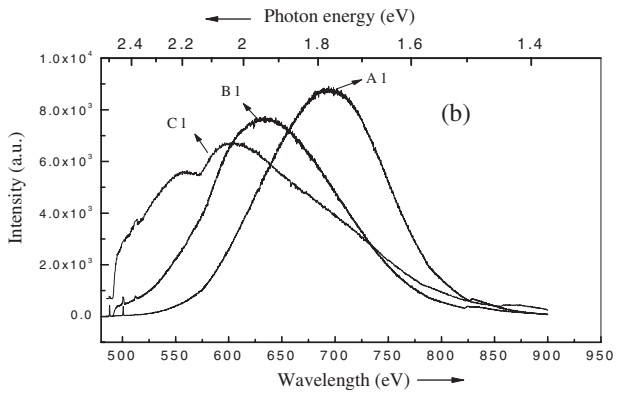

Figure 4. PL spectra of samples A1, B1, and C1, excited by the 488 nm line of an Ar^+ laser.

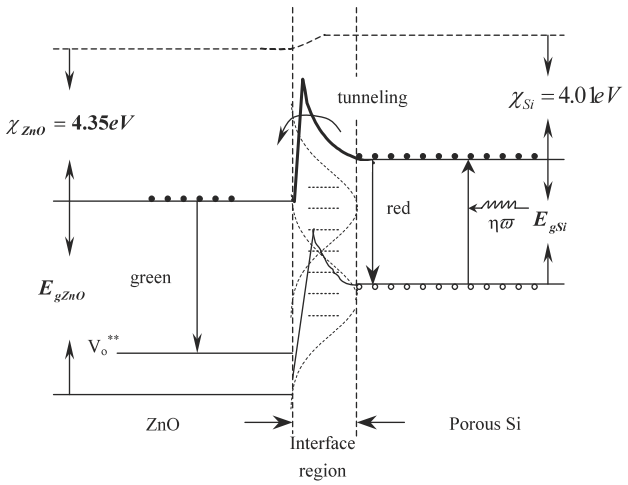

Figure 5. Schematic band diagram of the ZnO/porous Si composite, describing the emission mechanism.

that of c-Si (1.12 eV) due to the quantum confinement effect. The band gap of ZnO is $E_{gZnO} = 3.37$ eV. When the 488 nm line of an Ar^+ laser was applied to the composite system, only porous Si could be excited. The photoabsorption process occurred from the band gap of Si nanocrystals, widened by the quantum confinement effect. The red emission comes from the porous Si surface, modified by the deposited ZnO. The entire surface of the fresh porous Si is covered with hydrogen, such as in SiH_x species [9, 18], which are unstable when ZnO is grown on the surface. Si−H bonds would break and Si=O bonds form after ZnO deposition on the porous Si surface [10]. This can also been observed in the Raman spectra of the composite system. After deposition of ZnO, the Raman peak of the crystalline Si shifts to a high wave number of 520 cm^{-1}, which might be stress-induced shifts because oxidation brings compressive stress, which shifts the Raman peak to the high wave number [19, 20]. Wu *et al* [10] have shown oxidation of surface Si atoms will lead to a blueshift of the red emission from porous Si due to the additional potential modulation with the Si nanocrystallite by a long-range Coulomb interaction of oxygen ions. If the oxygen passivation of surface Si atoms is deeper, the surface Si atoms are attached by oxygen ions to form a dilute shell of oxygen. Due to the negative charge of this oxygen shell, the electrostatic potential of electrons in a Si shell near the surface will increase. This reduces the effective size of the Si nanocrystallites and enlarges the gap for the free excitons. Therefore, a blueshift of Si nanocrystallites due to the oxygen passivation becomes possible. With an increase in etching time, the size of Si nanocrystalline decreases and this leads to an increase in porous Si surface area. Therefore, more nano-Si atoms are passivated by oxygen ions, enlarging the blueshift of the red emission with the increase in porosity of porous Si.

Simultaneously, because of the large surface-to-volume ratio for nanocrystalline Si, a band bend is formed at the ZnO/porous Si interface. With an increase in the surface-to-volume ratio of porous Si, direct tunnel transfer of photoexcited carriers across the energy barrier from porous Si to the conduction of ZnO could be suggested due to narrowing of the barrier. The photogenerated carriers tunnelling to the ZnO conduction band then recombine with the V_0^{**} level deep in the band gap, causing emission of the green light. With the narrowing of the barrier caused by increasing the surface-to-volume ratio, the number of carriers tunnelling through the barrier increases, which results in enhancement of the green band intensity with the increase in template porosity. Therefore, the green emission of the composite system becomes more and more obvious from samples A1 to C1. The reason why the green emission band and the red emission band compete with each other can be easily understood since more carriers tunnel through the barrier to participate in the emission of the green band, and the carriers involved in the recombination of the red band become less. From the above discussion, this model is well consistent with the experimental results.

4. Conclusions

In conclusion, we present a photoluminescence study of ZnO grown on porous Si templates. A model was proposed to interpret the emission mechanism. The photoabsorption is from the band gap of Si nanocrystals, widened by the quantum confinement effect. The red emission band corresponds to the radiation of the oxygen-passivated porous Si surface after deposition of ZnO and the green emission band is due to the deep-level defect emission associated with the deep trap level of V_0^{**} in the ZnO band gap.

Acknowledgments

This work was supported by the Program of CAS Hundred Talents, the National Natural Science Foundation of China, No 60176003, the Innovation Foundation of CIOFP, Excellent Young Teacher Foundation of Ministry of Education of China, and the Foundational Excellent Researcher to Go beyond Century of the Ministry of Education of China.

References

[1] Wu X L, Siu G G, Fu C L and Ong H C 2001 *Appl. Phys. Lett.* **78** 2285
[2] Ko H J, Chen Y F, Zhu Z, Yao T, Kobayashi I and Uchiki H 2000 *Appl. Phys. Lett.* **76** 1905
[3] Ohtomo A, Tamura K, Saikusa K, Takahashi T, Makino T, Segawa Y, Koinuma H and Kawasaki M 1999 *Appl. Phys. Lett.* **75** 2635
[4] Zhang W H, Shi J L, Wang L Z and Yan D S 2000 *Chem. Mater.* **12** 1408
[5] Li Y, Meng G W, Zhang L D and Phillipp F 2000 *Appl. Phys. Lett.* **76** 2011
[6] Canham L T 1990 *Appl. Phys. Lett.* **57** 1046
[7] Xu D S, Guo G L, Gui L L, Tang Y Q, Shi Z J, Jin Z X, Gu Z N, Liu W M, Li X L and Zhang G H 1999 *Appl. Phys. Lett.* **75** 481
[8] Chin V, Collins B E, Sailor M J and Bhatia S N 2001 *Adv. Mater.* **13** 1877
[9] Wolkin M V, Jorne J, Fauchet P M, Allan G and Delerue C 1999 *Phys. Rev. Lett.* **82** 197
[10] Wu X L, Xiong S J, Fan D L, Gu Y, Bao X M, Siu G G and Stokes M J 2000 *Phys. Rev.* B **62** R7759
[11] Liu Y L, Liu Y C, Liu Y X, Shen D Z, Lu Y M, Zhang J Y and Fan X W 2002 *Physica* B **322** 31
[12] Mavi H S, Shukle A K, Abbi S C and Jain K P 1989 *J. Appl. Phys.* **66** 5322
[13] Kanemitsu Y, Uto H, Masumot Y, Matsumoto T, Futagi T and Mimura H 1993 *Phys. Rev.* B **48** 2827
[14] Elhouichet H and Oueslati M 2001 *Mater. Sci. Eng.* B **79** 27
[15] Maruyama T and Ohtani S 1994 *Appl. Phys. Lett.* **65** 1346
[16] Zhang Y H, Li X J, Zheng L and Chen Q W 1998 *Phys. Rev. Lett.* **81** 1710
[17] Dijken A V, Meulenkamp E A, Vanmaekelbergh D and Meijerink A 2000 *J. Phys. Chem.* B **104** 1715
[18] Rao A V, Ozanam F and Charzalviel J N 1991 *J. Electrochem. Soc.* **138** 153
[19] Weinstein B A and Piermarini J 1975 *Phys. Rev.* B **12** 1172
[20] Yamada M and Kondo K 1992 *Japan. J. Appl. Phys.* **31** L993